Investigation and Validation of Methods to Implement a Two-Quadrant Battery Emulator for Power Hardware-in-the-Loop Simulation

Nikolaos Daniil and David Drury
Department of Electrical and Electronic Engineering
University of Bristol
Bristol, UK
nikos.daniil@bristol.ac.uk, d.drury@bristol.ac.uk

***Abstract*—When new hardware is developed, it is often convenient to test the prototype in a Hardware-in-the-Loop Simulation (HILS). In this technique, the critical parts of the system including the hardware-under-test (HUT) are physically present while the rest of the system is emulated in real time. In this paper, a battery emulator (BE) is implemented to replicate the behaviour of a battery pack in a HILS experiment. For this purpose, a remotely controlled DC power supply is used, combined with external passive elements to allow two-quadrant operation. The emulation fidelity is validated through experimental comparison with a real battery pack under constant and pulsed current loads. These experiments show the importance of the impedance connecting the BE to the HUT and how a poor selection can cause oscillations that would not exist in an experiment with a real battery pack.**

Keywords*—*Power Hardware-in-the-Loop Simulation; battery emulator; battery modelling; voltage response; emulation fidelity

I. Introduction

This paper investigates methods to implement a battery emulator (BE) capable of two-quadrant operation (charging and discharging), using a unidirectional remotely controlled DC source. Instead of designing and building a tailor-made hardware, it is decided to use off the shelf equipment. This is done in order to demonstrate how a BE can be implemented easily, using equipment available in any Power Electronics Lab and how the challenges encountered can be overcome.

When developing battery packs and associated hardware, engineers have two main options. They can either test the entire system (battery, converter, electric drive etc) together once each component is available and complete, or test each of the components in isolation. The first option provides more reliable results but it requires all aspects of the final design to be in place. This task is impractical, especially for batteries as they can be expensive and bulky. They also demand a management system for protection and require a long initialization procedure. Thus, the second option is often followed in which the battery pack is replaced by a stiff voltage source. However, this choice results in tests that miss some aspects. Batteries are non-linear devices and their voltage and output impedance depend not only on the present operational conditions but also on how they were treated in the past. Moreover, due to the highly interactive behaviour of the full system, the dynamics will possibly be different to those of a real battery pack.

An intermediate solution is to perform the tests using the method of Hardware-in-the-Loop Simulation (HILS). In this technique the critical part of the equipment is physically present while the rest of the system is simulated in real time. Depending on the way the real hardware interacts with the simulated equipment, the simulation can be implemented on a Signal (or Control), a Power or a Mechanical level [1].

The emerging questions are how accurately a BE can replicate the behaviour of a real battery pack and how it is ensured that the measured dynamics are caused by the hardware-under-test (HUT) and not by the BE. In order to answer these questions, it is necessary to focus on the internal structure of the original setup and compare it with the Power HILS (PHILS) setup as seen in Fig. 1. Potential error sources in the described PHILS setup are:

- Measurement errors.
- Battery modelling errors.
- Errors in the BE-HUT power interface.

An example of the magnitude of measurement and modelling errors can be found in [2]. In this work, it is assumed that the measurements have zero error offset and the battery model is accurate. The problem then is localized on the power interface and on how a BE can follow with fidelity and stability the reference voltage set by the battery model.

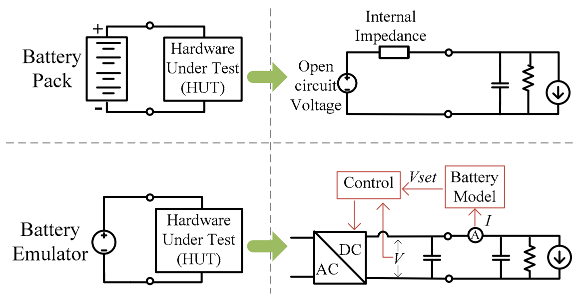

Fig. 1. Testing a new hardware with a real battery pack and in a PHILS environment using a BE.

This work is sponsored by the Bristol University Alumni Foundation with a grant kindly provided by Dr. Gerald Avison.

The BE behaviour is compared with an original battery pack consisting of one branch with 12 cells in series and the emulation fidelity is verified. The fundamental cell used is the 1250-mAh polymer Li-ion VARTA LPP 503562 DL [3].

II. System Description

A. Battery Model

Among the battery models found in the literature, the circuit-based model developed in [2] is chosen which is shown in Fig. 2. The reasons for selection are the simple parameterisation procedure in the time domain and the low computational effort required to be executed by the real-time platform. The circuit-based model consists of a voltage source in series with a resistance and a ladder of two RC networks. For the VARTA LPP 503562 DL cell, the first RC network has a time constant in the range of tens of seconds and the second one a range of hundreds of seconds [2]. Consequently, the battery model response to effects with a time scale less than 100 ms practically depends solely on the value of the voltage source V_{int} and the series resistance R_{int} which are estimated as functions of state of charge (*SoC*). According to [2], the series resistance for the cell used can take values from 0.12 Ω to 0.26 Ω per cell, meaning 1.44 Ω to 3.12 Ω for the 12-cell series configuration.

B. Real-Time Platfrom

The real-time platform used is the dSpace DS1104 R&D Controller Board, programmed in Simulink environment using the ode1 solver as shown in [2]. The tasks performed are current input, execution of the battery model, estimation of the voltage that a real battery pack would have, performance of some supplementary control actions if required and finally output of the reference voltage to the power device. The execution time step is chosen to be 40 μs to offer a safety margin compared to 22 μs that is the minimum time required to execute a battery model with constant RC elements. Apart from controlling the power device, the dSpace DS1104 offers a graphical user interface (GUI) which facilitates the supervision of the experiments.

C. Power Device

The device chosen to implement the BE is the Delta Elektronika SM 52-AR-60 power supply [4]. Apart from availability, the reasons for its selection are that it has the desired power rating and it can be remotely controlled via an analogue interface without the interference of any internal sampler that could increase the delay. Moreover, it provides current and voltage readings which can be processed by the real time platform. The major disadvantage is that it does not natively support current sinking operation. For this reason, a current sink resistor is used in parallel with the voltage terminals as shown in Fig. 3. When the device has to emulate charging behaviour, the current coming from the HUT will go through the R_{sink}. The series diode is used only for protection and it should remain forward biased. This way, the power supply will always source current and consequently dictate the voltage in the power interface. Thus, R_{sink} should fulfil the condition:

$$R_{sink} \cdot I_{charge}^{max} \cdot b < V_{cell}^{min} \cdot n - V_D \tag{1}$$

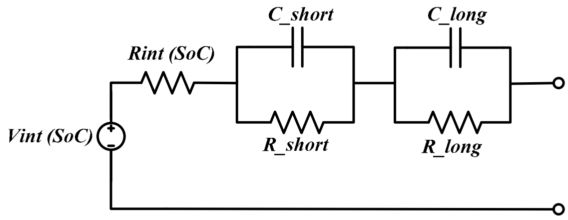

Fig. 2. The circuit-based battery model used in [2].

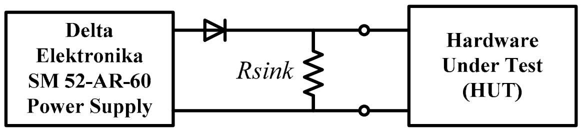

Fig. 3. Connecting the Delta Elektronika power supply in a configuration for achieving two-quadrant operation for the battery emulator.

Where:

n	number of fundamental cells connected in series, n=12 for the specific design
b	number of cell branches connected in parallel, b=1 for the specific design
I_{charge}^{max}	maximum cell charging current
V_{cell}^{min}	minimum allowable cell voltage
V_D	diode voltage drop

For the fundamental cell used, the manufacturer's data are I_{charge}^{max}=1.25A and V_{cell}^{min}=3V [3] meaning that R_{sink} < 28.8 Ω.

In order to understand the dynamics of the selected power supply, a model has been derived for operation in voltage control mode which is shown in Fig. 4. The basic components of the model are a DC voltage source controlled by a PI controller which charges the output capacitor through the series resistance R_1. If there were no other elements, the system would have been linear but this is not the case. The diode prevents the capacitor from being discharged through the internal voltage source. Consequently, when a voltage decrease is demanded, the capacitor can only be discharged through the built-in resistor R_2 and the externally connected hardware. This behaviour is presented in Fig. 5a. Another nonlinearity is introduced by the current limiter. After a voltage increase is requested, the capacitor has to be charged to reach the required voltage. When the current of the internal voltage source exceeds the value of 30A, a current limiter is activated. The activation of the current limiter is presented in Fig. 5c while a voltage increase that does not activate it is shown in Fig. 5b.

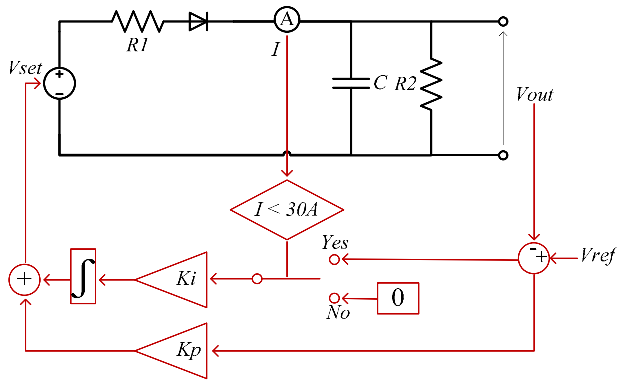

Fig. 4. The model derived for Delta Elektronika SM 52-AR-60 operating in voltage control mode.

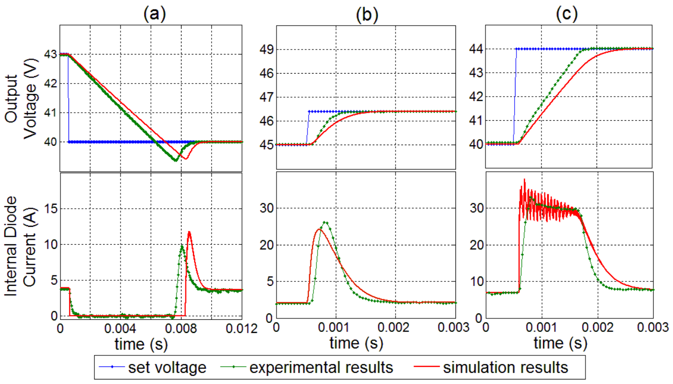

Fig. 5. The measured and modelled response of Delta Elektronika SM 52-AR-60 when operating in voltage control mode and the reference voltage changes. Part (a) shows the response to a set voltage decrease, (b) shows a voltage increase in which the current limiter is not activated and (c) shows a voltage increase with activation of the current limiter.

As a result of the two nonlinearities described above, adding an external controller stage will have limited benefits in offering a higher response bandwidth. For this reason, it is decided to use external circuit elements in an attempt to compensate for the slow response.

III. Emulator Response in Step Resistive Load Changes

The emulator's fidelity in step resistive load changes is verified by comparing its behaviour with a real battery pack. The comparison experiments are conducted in low power against a single branch of 12 VARTA cells [3] in series. The emulator's voltage is dictated by a battery model which, as explained in Section II/A, has been simplified to a voltage source with a series resistance for timescales less than 100 ms. Since the comparison experiments last for a very short time, it can be assumed that the *SoC* does not change and thus the voltage and resistor values remain constant. The first set of experiments involve connecting directly the power supply to the load as presented in Fig. 6a (D connection). The emulator's voltage response in a step decrease and increase of the load resistance is presented in Fig. 7. In this figure, the voltage estimated by the battery model and the voltage of the real battery pack are also shown.

An important matter to explain is why there is a difference between the experimental and the modelled voltage response. This happens due to the sampler that is used for the model parameter extraction in [2]. The sampler there is 100 ms meaning that all the dynamics with lower time constant are ignored. It would then be more accurate to use a lower value for the battery model series resistance R_{int} and add a third RC circuit with a time constant of tens of milliseconds. However, modifying a battery model is outside the scope of this paper. Thus, for the comparisons to follow, the voltage resulting from the existing model will be considered accurate.

The first thing to observe in Fig. 7 is that when the output voltage drops, the duration of the transition can be long. This happens due to the nonlinear behaviour introduced by the internal diode as explained in Section II/C. On the contrary, the transition is much quicker when the output voltage has to rise. This happens because the total output current is low and there is an adequate margin up to the 30-A threshold.

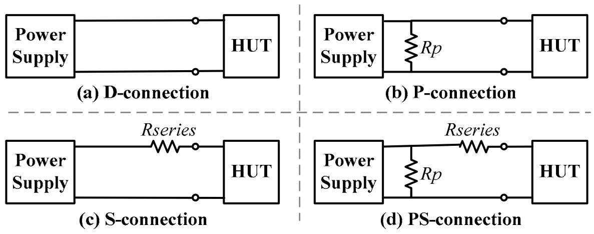

Fig. 6. The tested battery emulator output impedance topologies with the hardware under test being a resistive load.

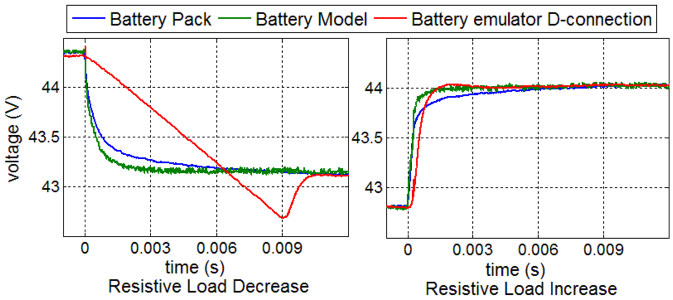

Fig. 7. Experimental, modelled and emulated voltage response to step resistive load changes.

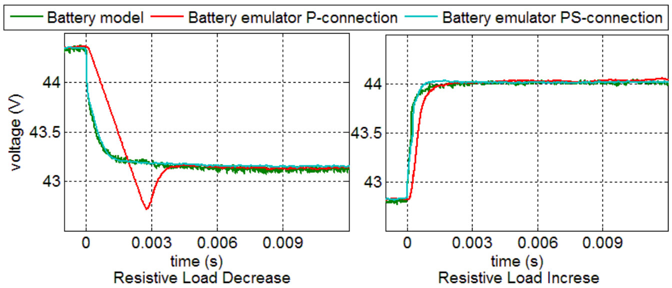

Fig. 8. Comparison of the emulator topologies presented in Fig. 6b (P-connection), Fig. 6c (S-connection) and 5d (PS-connection) based on their performance in step resistive load changes. The resistor values used are R_p = 13.8 Ω and R_{series} = 1 Ω.

Since the problem is related with the discharge of the output capacitor, it could be solved by using a resistor R_p in a parallel branch as presented in Fig. 6b (P connection). This resistor has a dual role. It allows two-quadrant operation as shown in Section II/C and helps the output capacitor of the power supply to discharge faster. Thus, the condition $R_p < R_{sink}^{max}$ should be fulfilled. The emulator's behaviour with this configuration is presented in Fig. 8. It can be seen that the voltage drop transition takes less time than before while the deterioration in the voltage increase transition is not significant.

Another method considered for improving fidelity is to use a series resistor R_{series} to emulate the R_{int} of the battery model. The difficulty in this approach is that the value of R_{int} is not constant. As shown in Section II/A, R_{int} varies between 0.12 Ω and 0.26 Ω per cell, meaning 1.44 Ω to 3.12 Ω for a 12-cell, single branch configuration. During the experiments, the measured value of R_{int} using a 100-ms sampler is 1.51 Ω. The chosen value of R_{series} is 1 Ω because the emulation fidelity should be shown for the general case in which $R_{series} \neq R_{int}$. As illustrated in Fig. 8, the transition during the voltage drop is quicker than that of the D-connection. Finally, a third topology is tested in Fig. 8 which includes both series and parallel resistors as presented in Fig. 6d (PS connection) and which shows the best behaviour.

IV. EMULATOR RESPONSE IN PULSED CURRENT LOAD

A. Pulsed Current Load

The analysis of the BE behaviour in step resistive load changes shows roughly the advantages and disadvantages of each topology but it does not correspond to the realistic conditions that the BE will be operated. As described in the introduction, BEs are used to test new prototype hardware which usually are switched devices operating like pulsed current loads. The device chosen to represent the HUT is the half-bridge DC/DC converter with a hysteresis current control loop developed in [5] and shown in Fig. 9.The BE is connected to the high side of the converter.

B. Experimental Results

The battery pack voltage and current ripple when connected to the high side of the half-bridge converter are shown in Fig. 10. In Fig. 10a the average battery pack current is 0.25 A while in Fig. 10b it is 1 A. In the latter case, the frequency is also increased because the converter uses a hysteresis control loop. In Fig. 11 the same experiments are shown when replacing the battery pack with a BE P-connection with $R_p = 13.8\ \Omega$. While the emulation in Fig. 11a has relatively low fidelity but no oscillations, when the current and the frequency are increased, the system starts to oscillate as shown in Fig. 11b and the emulator totally fails to replicate the battery's behaviour. Using a parallel resistor R_p of lower value makes the situation worse as the system has been observed to start oscillating at a lower current than before. The emulation results are much improved when a series resistor $R_{series} = 1\Omega$ is added as in the PS-connection as shown in Fig. 12.

In total, the PS connection shown in Fig. 6d having both series and parallel resistors is selected. The parallel resistor has been observed to cause oscillations but it is necessary in order to emulate the charging behaviour. As a result, its value will be the highest possible according to (1). The selected value is $R_p = 25\ \Omega$ so that $R_p < R_{sink}^{max} = 28.8\ \Omega$. Concerning the series resistance, a compromise is required. A very low value could be insufficient to supress the oscillations while a high value would cause elevated ohmic losses. Finally, the value $R_{series} = 1.6\ \Omega$ is selected. An analysis on the requirements that R_{series} needs to obey can be found in [6].

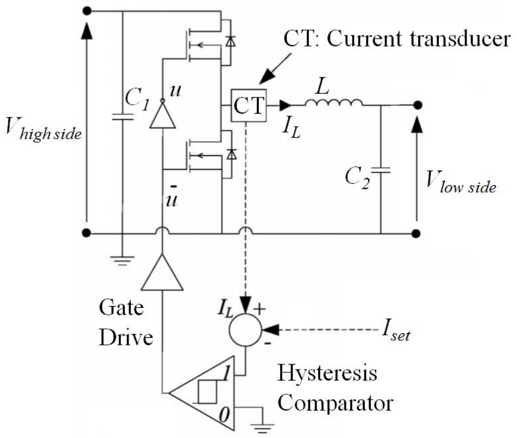

Fig. 9. The half-bridge DC/DC converter with hysteresis control loop used for the pulsed current load experiments [5].

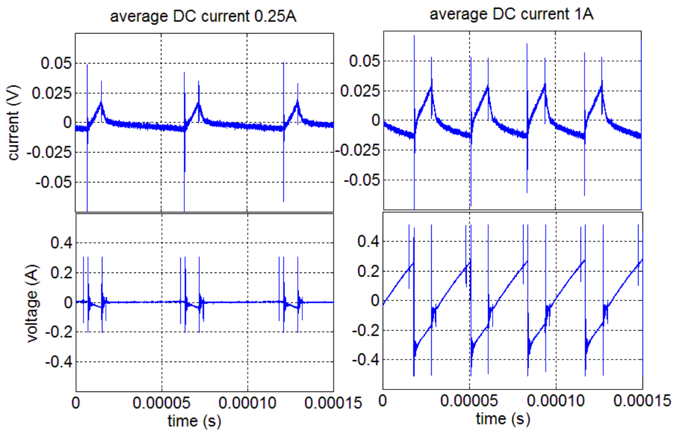

Fig. 10. Current and voltage ripple of the battery pack while connected in the high side of the half-bridge converter of Fig. 9. Discharging operation is shown.

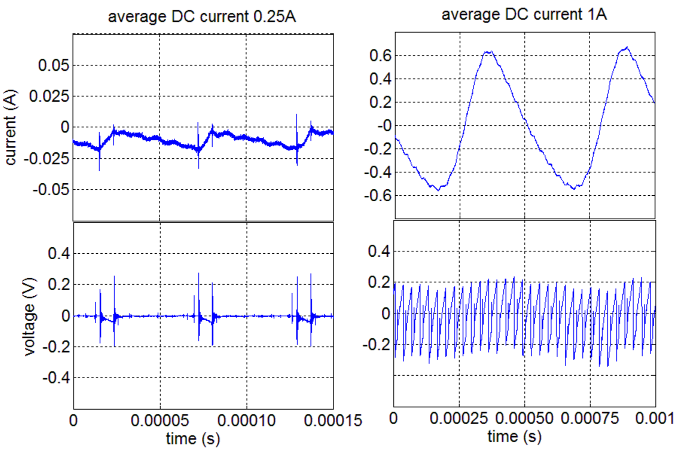

Fig. 11. Current and voltage ripple of the BE connected to the high side of the half-bridge converter of Fig. 9 using the P-connection with $R_p = 13.8\ \Omega$. Discharging operation is emulated.

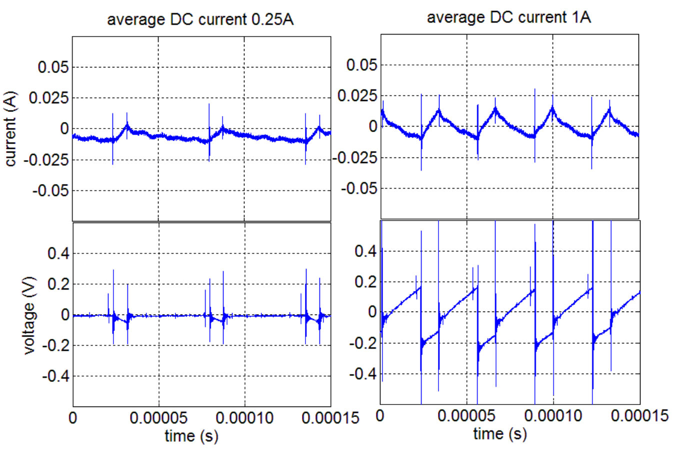

Fig. 12. Current and voltage ripple of the BE connected to the high side of the half-bridge converter of Fig. 9 while using the PS-connection with $R_p = 13.8\ \Omega$ and $R_{series} = 1\ \Omega$. Discharging operation is emulated.

V. EMULATION IN CHARGING AND IN COMBINED CYCLES

For emulation of the charging behaviour, a current sink resistor is used as explained in Section II/C and shown in Fig. 3. Thus, the only difference between charging and discharging operation is a constant DC offset current that the power source has to supply during charging which is given as:

$$I_{DC\ offset} = \frac{V_{Delta} - V_D}{R_{sink}} - I_{charging} \quad (2)$$

Where:

V_{Delta} voltage in the output terminal of the Delta Elektronika power supply

V_D diode voltage drop

R_{sink} current sink resistor of Fig. 3

$I_{charging}$ charging current taking only positive values. During discharging it is equal to zero

A comparison between the real and the emulated voltage response to step changes of charging current is illustrated in Fig. 13. The current and voltage ripple when the half-bridge converter of Fig. 9 is in charging mode is shown in Fig. 14 for both the real battery pack and the BE.

Having shown that the emulator operates without oscillations and with good fidelity both in charging and discharging operation, the overall accuracy of the emulator needs to be demonstrated. For this purpose, a scaled version of the power profile PHEV20 [7] is used which consists of both charging and discharging phases. The half-bridge converter of Fig. 9 is used for this purpose with the BE or the battery pack connected to the high side. The battery pack and BE voltages are presented in Fig. 15. For the 360 s of emulation, the measured root mean square error between the battery pack and the battery model is 45.8 mV (3.8 mV / cell), between the battery model and the BE is 60 mV (5 mV / cell) and the total error between the battery pack and the BE is 83.9 mV (7 mV / cell).

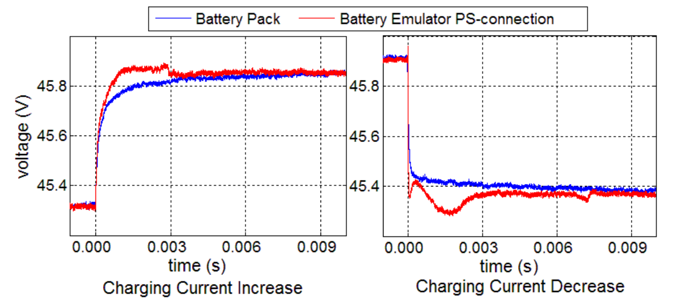

Fig. 13. Battery pack and battery emulator in PS connection voltage response to step change of the charging current.

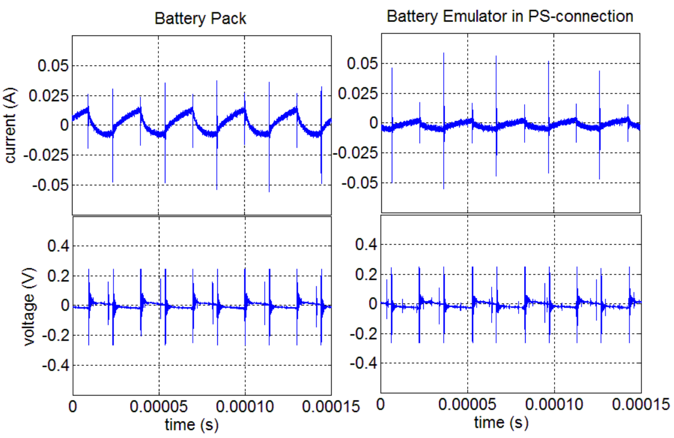

Fig. 14. Voltage and current ripple of the battery pack and battery emulator in PS connection connected to the high side of the half-bridge converter of Fig. 9. Charging behaviour is studied with an average current value of 1A.

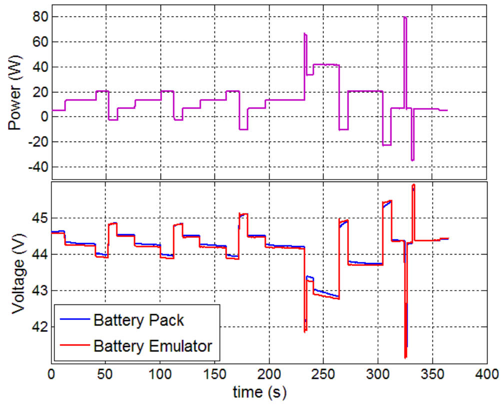

Fig. 15. Battery pack and battery emulator voltages when connected to the high side of the half-bridge converter of Fig. 9 while the low side implements a scaled-down version of the PHEV20 power profile [7]. Positive power corresponds to discharging operation.

VI. Related Work

A. Battery Modelling

The battery model used to estimate the emulator reference voltage is circuit-based as explained in Section II. Circuit-based models are intuitive, demand relatively low computational power and are generally easy to parameterize in the time domain [2]. An alternative method is to parameterize the model in the frequency domain using impedance spectroscopy as shown in [8]. In the model presented there, the RC networks are replaced with constant phase elements (CPE) and a Warburg impedance is added in series. As these elements are parameterized in the frequency domain, this model gives a more accurate estimation of the battery impedance as a function of the ripple frequency. The option of using a model like this was considered but finally rejected because CPEs demand 1.8 to 4 times higher computational power to be executed [9] meaning that a slower sampler needs to be used.

B. Power Interface

The problem of stabilizing the emulator – HUT interface has been studied in the past and several approaches have been proposed both in software and in hardware level. In [10] a comparison of five different interface algorithms is presented to provide a guide on how to select the type of signals to be transmitted and the method to process them. One of the methods presented is the Ideal Transformer Model (ITM) which is the one applied in the present paper. The described ITM interface is shown in Fig. 16 in which the non-ideality of the power device is simulated as an external disturbance ε. When this error is fed back in the model, it creates a further error of [10]:

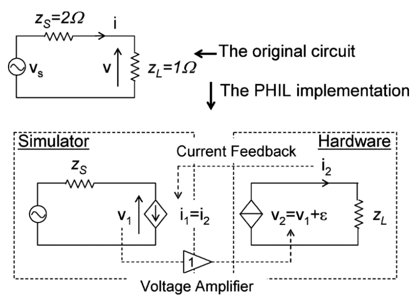

Fig. 16. The ideal transformer model (ITM) for the emulator power interface described in [10].

$$\Delta v_1(t_{k+1}) = -\left(\frac{z_S}{z_L}\right)\varepsilon \tag{3}$$

The system is unstable for $z_S > z_L$ because the error is amplified after each time step. Using a real resistor to emulate a part of the battery internal resistance can be seen as a method to decrease the value of z_S, increase z_L and bring the whole system inside the stable region. Another example of how some of the interfaces of [10] can be used in practice can be found in [11] where the emulated system is the distribution network and the HUT are photovoltaic inverters.

The technique of using passive circuit elements between the emulator and the HUT in order to increase the emulation fidelity can also be applied when more dynamic systems like machines drives are tested in a Power HILS. In [1] the performance of two interface filters connecting the HUT with a machine emulator are compared. It is concluded that using an LCL filter with Model Predictive Control (MPC) is preferable to using an L filter with PI control.

C. Battery Emulators

An example of how the ITM method of [10] can be applied in battery emulation is presented in [12]. In that study, a bidirectional power device is used for the implementation of the emulator. As a result, there is no need for a current sink resistor. The important difference between [12] and the present paper is that in [12] there is a real series resistor in the input of the HUT. As a result, the problem of connecting a low output impedance emulator to a low input impedance HUT does not exist and instability issues or oscillations do not occur.

A different and holistic approach on using a BE in a Power HILS is proposed in [13]. The problem of low output impedance of the device implementing the emulator is located but the solution proposed is in control level. In the method presented, the models of the battery, BE and the HUT are combined in one configuration and model predictive control (MPC) is used to achieve robust impedance control of the whole system.

While in most cases the battery pack is emulated as a whole like in [13] and [12], there are examples in which the emulation has to be done in cell level. Using a different emulator for each cell inevitably increases the complexity and the overall cost but it may be necessary when the HUT is a battery management system (BMS). A typical example is [14] in which cell level emulation is applied in order to test a cell balancing circuit.

VII. Conclusion

Replacing a battery pack with a BE in a Power HILS facilitates the testing of new hardware but it could lead to erroneous results because the devices used to implement battery emulators have different dynamics to the real batteries. This paper describes a simple method of implementing a two-quadrant battery emulator using an off-the-shelf remotely controlled power source. Since the power supply used is unidirectional, a parallel resistor is placed on its terminals to allow current sinking operation. This parallel resistor also reduces the time of voltage drop transitions because it helps the output capacitor of the power supply to discharge faster.

The BE behaviour is compared with a real battery pack showing high fidelity for resistive loads. For pulsed current loads, the experiments showed that the BE-HUT power interface is possible to perform unwanted oscillations that heavily distort the emulation. These oscillations can be supressed when a series resistor is placed between the BE and the HUT partly replicating the behaviour of the battery output impedance. The configuration proposed with series and parallel resistors shows the highest fidelity for emulating both charging and discharging operations. Details on the mechanism causing the oscillations and the reason why the intuitive solution proposed succeeds in supressing them are given in [6].

References

[1] S. Lentijo, S. D'Arco, A. Monti, "Comparing the Dynamic Performances of Power Hardware-in-the-Loop Interfaces," *IEEE Transactions on Industrial Electronics*, vol.57, no.4, pp.1195-1207, April 2010.

[2] N. Daniil, D. Drury, P.H. Mellor, "Performance Comparison of Diffusion, Circuit-based and Kinetic Battery Models," *Energy Conversion Congress and Exposition (ECCE), 2015 IEEE*, pp.1382-1389, 20-24 Sept. 2015.

[3] VARTA, "LPP 503562 DL", 56422201012 datasheet, June 2008.

[4] Delta Elektronika, "Manual SM1500N.vp", Rev. Oct. 2015.

[5] A. M. Gee, F. V. P. Robinson, R. W. Dunn, "Analysis of Battery Lifetime Extension in a Small-Scale Wind-Energy System Using Supercapacitors," *IEEE Transactions on Energy Conversion*, vol. 28, no. 1, pp. 24-33, March 2013.

[6] N. Daniil, D. Drury, "Improving the Stability of the Battery Emulator – Pulsed Current Load Interface in a Power Hardware-in-the-Loop Simulation", *Industrial Electronics Society, IECON 2016 – 42nd Annual Conference of the IEEE*, accepted for publication.

[7] Idaho National Laboratory, "Battery Test Manual For Plug-In Hybrid Electric Vehicles," Rev. 3, INL/EXT-14-32849, Sep. 2014.

[8] S. Buller, M. Thele, R.W. De Doncker, E. Karden, "Impedance-based simulation models of supercapacitors and Li-ion batteries for power electronic applications," *IEEE Transactions on Industry Applications*, vol.41, no.3, pp.742-747, May-June 2005.

[9] D. Andre, M. Meiler, K. Steiner, H. Walz, T. Soczka-Guth, D.U. Sauer, "Characterization of high-power lithium-ion batteries by electrochemical impedance spectroscopy. II: Modelling," *Journal of Power Sources,* vol.196, iss.12, pp.5349-5356, June 2011.

[10] W. Ren, M. Steurer, T.L. Baldwin, "Improve the Stability and the Accuracy of Power Hardware-in-the-Loop Simulation by Selecting Appropriate Interface Algorithms," *Industrial & Commercial Power Systems Technical Conference, ICPS 2007. IEEE/IAS*, pp.1-7, 6-11 May 2007.

[11] A. Viehweider, F. Lehfuss, G. Lauss, "Interface and Stability Issues for Siso and Mimo Power Hardware in the Loop Simulation of Distribution Networks with Photovoltaic Generation," *International Journal of Renewable Energy Research (IJRER)*, vol. 2, no. 4, pp. 631–639, 2012.

[12] C. Seitl, J. Kathan, G. Lauss, F. Lehfuss, "Power hardware-in-the-loop implementation and verification of a real time capable battery model," *2014 IEEE 23rd International Symposium on Industrial Electronics (ISIE),* Istanbul, 2014, pp. 2285-2290.

[13] O. Konig, C. Hametner, G. Prochart, S. Jakubek, S., "Battery Emulation for Power-HIL Using Local Model Networks and Robust Impedance Control," *IEEE Transactions on Industrial Electronics*, vol.61, no.2, pp.943-955, Feb. 2014.

[14] Wai Chung Lee, D. Drury, "Development of a Hardware-in-the-Loop Simulation System for Testing Cell Balancing Circuits," *IEEE Transactions on Power Electronics*, vol.28, no.12, pp.5949-5959, Dec.2013.